이화여자대학교 대학원
2024학년도
석사학위 청구논문

Kinodynamic Simulation of Extreme-Density Crowds: A Case Study on the Itaewon Disaster

인공지능·소프트웨어학부

Juyi Hwang

2025

Kinodynamic Simulation of Extreme-Density Crowds: A Case Study on the Itaewon Disaster

이 논문을 석사학위 논문으로 제출함

2024 년 12 월

이화여자대학교 대학원

인공지능·소프트웨어학부 Juyi Hwang

Juyi Hwang의 석사학위 논문을 인준함

지도교수 김영준 _____

심사위원 박상수 _____

오유란 _____

김영준 _____

이화여자대학교 대학원

Table of Contents

List of Figures

List of Tables

Abstract

We present novel crowd simulation methodologies designed to virtually reenact the Itaewon disaster that occurred in 2022 as a result of extreme crowd density. This dissertation addresses the limitations of conventional techniques, which struggle to effectively simulate a variety of crowd behaviors seen during incidents of extreme density, including crowd surges, fluidization, and crowd collapse. To overcome these challenges, we introduce a kinodynamic simulation that integrates four distinct types of agents: kinematic agents for representing low-density crowd behaviors, hydrodynamic and hydrostatic agents for simulating high-density crowds, and articulated passive agents to model individuals in dense contact environments. These heterogeneous agent types interact through a message-passing mechanism that enables the sharing of kinematic and dynamic data, facilitating smooth agent-type transitions based on crowd density and contact forces.

The proposed hybrid simulation method demonstrates an ability to accurately replicate the crowd behaviors observed during the Itaewon incident compared to actual CCTV footage. Our experimental results reveal that the kinodynamic agent model successfully captures the complex behaviors associated with extreme crowd densities, providing key insights into the advantages of using hybrid agents to represent various crowd phenomena. Additionally, we present an ablation study to analyze the contribution of each agent type, confirming the critical role of kinodynamic agents in enhancing the accuracy of extreme-density crowd simulations. Furthermore, we conducted three what-if scenario simulations, proposed by disaster management experts, to evaluate how various interventions might prevent the Itaewon disaster. The scenarios explored measures such as controlling the influx of people, implementing right-hand traffic, and removing illegal structures within narrow alleyways. Our findings indicate that a combination of these strategies significantly improves crowd flow and minimizes the risk of dangerous crowding. To further demonstrate the versatility and applicability of our proposed methods, we extended our simulations to replicate two other real-world crowd incidents: the Love Parade 2010 and

the Oasis Concert 2005. These replications illustrate the applicability of the hybrid simulation framework in diverse crowd situations, highlighting its potential as a tool for predicting crowd patterns and designing proactive crowd safety management strategies for large-scale gatherings.

I. Introduction

A. Background

On October 29, 2022, a large crowd gathered in Itaewon, Seoul, Korea, to celebrate the Halloween festival. The estimated number of people was $130k$, which was significantly higher than in previous years. After 6 pm, crowds began to gather and become congested in the alley in front of Itaewon Station. The alley was the shortest route to World Food Culture Street, attracting large groups of people who tried to move through it simultaneously. Despite the congestion and the ongoing influx of people creating a risky situation, no appropriate measures were taken. Eventually, around 10:15 pm, a significant number of pedestrians fell into the alley, resulting in 158 deaths and 320 injuries.

Several reports attribute the cause of the accident to several intertwined factors [11, 22, 33]. Firstly, 2022 was the first year since the COVID-19 pandemic began that social distancing restrictions were relaxed, which had previously been in place for nearly three years. As a result, the festival was held after a long time, and more people who were eager to return to social activities came to Itaewon to enjoy Halloween. On the day of the accident, the population in the Itaewon area surpassed 36,000 within 300 meters of the accident site [2], marking the highest number since data collection began in 2017 [21]. Secondly, no appropriate crowd control measures were taken that day. As Halloween in Itaewon is an event without a designated organizer, participants gather spontaneously, and thus, local authorities must assess the event's scale and prepare effective safety measures. Despite this, traffic control or subway station closures to manage the large influx of attendees were not implemented, and the crowds continued to grow until the accident occurred [11, 22, 33]. Moreover, while the police were aware of the event, their preparations focused primarily on general security rather than crowd management. Consequently, despite 11 reports of crowd crush risks between 6 pm and 10 pm on the day, appropriate crowd control was not implemented by the police [18, 22].

In addition to administrative shortcomings, the characteristics of the alley contributed significantly to the disaster. The alley was narrow, ranging in width from $4.95m$ at its widest to just $3.20m$ at its narrowest, and had a slope ranging from 8.847° to 11.197°, as shown in Figure 1.1. This path was a quick shortcut lined with popular pubs, leading many people to take this route without being fully aware of the risks. At the T-shaped intersection that connects the accident alley to World Food Culture Street, high crowd density led to the fluidization of the crowd, meaning individuals were no longer able to move of their own accord. This situation ultimately caused the crowd density near the accident site to rise to 16 people per square meter (P/m^2), leading to crowd collapse and resulting in numerous casualties [2, 22, 33].

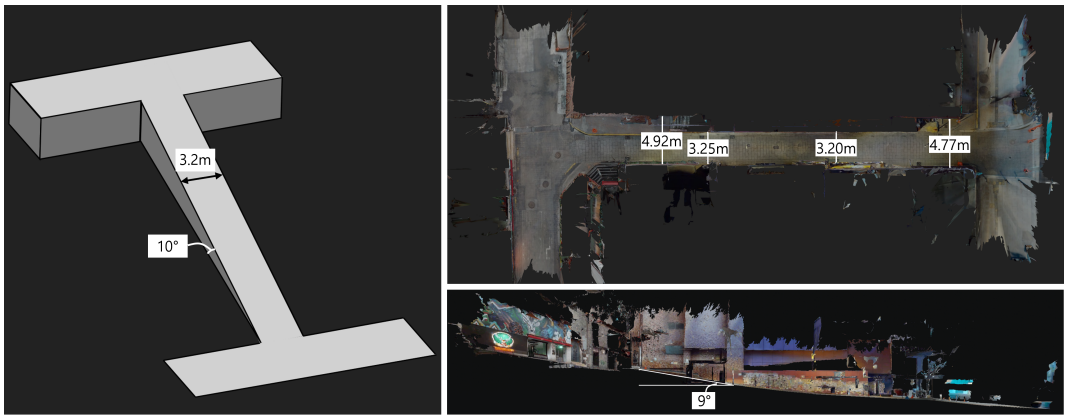

Figure 1.1. Itaewon 3D model and geographical characteristics

Furthermore, large events involving high-density crowds, such as concerts and festivals, have become more common in modern times, consequently increasing the risk of crowd-related accidents. Therefore, understanding crowd dynamics and establishing proactive crowd management strategies to prevent these incidents have become essential.

B. Research Objectives and Contributions

The goal of this dissertation is to find a realistic yet computationally efficient method to simulate the behavior of extremely dense crowds, such as in the Itaewon disaster, in order to reenact what could have happened in such a situation and to suggest a computational tool for relevant authorities to take preventive measures to avoid such disasters in the future.

A dense crowd is typically defined as having a density between four to six individuals per square meter (P/m^2) [1, 3, 20, 23, 26]. This dissertation defines extreme-density crowds as those with densities exceeding four P/m^2. Conventional high-density crowd simulation methods, such as continuum-based models [9, 10] and particle-based approaches [26, 34], struggle to effectively capture individual behaviors and accurately represent different crowd density levels. Additionally, in extreme-density conditions, complex phenomena such as crowd fluidization, surges, and collapses can emerge. However, existing methods are insufficient to fully capture and simulate all of these behaviors. This limitation makes it challenging to reproduce incidents like the Itaewon disaster adequately.

In this dissertation, we propose a new hybrid approach of kinodynamic simulation methods that utilize kinematic, hydrodynamic, and articulated-body dynamic agents to represent high-density crowds and reenact the Itaewon disaster accurately. We use kinematic agents for efficient obstacle avoidance and navigation in low density. We also employ hydrodynamic and hydrostatic agents to represent fluid-like phenomena and articulated passive agents to represent crowd collapses in high density. The main contributions of this dissertation can be summarized as follows:

- **Novel Co-Simulation Methods for Extreme-Density Crowd Behaviors**: We propose new co-simulation methods that cover various behaviors such as crowd surges, crushes, and collapses observed in the Itaewon disaster.
- **Hybrid Agent Model for Different Crowd Density Levels**: We develop a kinodynamic agent model incorporating kinematics, hydrodynamics, and rigid-body dynamics to effec-

tively represent crowd motion across different density levels. We also introduce a novel transition model between these heterogeneous agents, leveraging crowd density and contact forces inspired by real-world scenarios.

- **Reenactment of Itaewon Disaster Using Hybrid Agents**: By comparing our simulation results with public Itaewon CCTV footage, we demonstrate that our hybrid agent model can accurately replicate crowd behaviors and dynamics observed during the Itaewon disaster.
- **Ablation Study for Hybrid Agents**: We conduct an ablation study to validate the use of hybrid agents in reconstructing Itaewon crowd behavior, providing insights by analyzing the impact of each agent type on crowd density representation.
- **What-If Scenario Simulations**: We simulate three what-if scenarios based on our crowd modeling techniques to illustrate the potential of our approach for predicting crowd behavior and supporting the implementation of crowd accident prevention strategies in future events.
- **Simulation of Real-World Crowd Accidents**: We extend our simulations to two additional real-world crowd incidents to showcase the applicability of our simulation methods to different environments and scenarios.

C. Organization

The remainder of this dissertation proceeds as follows. In Chapter II, We review the previous works on crowd simulation and reenactment of crowd accidents. Chapter III introduces the modeling of environments and agents for three-dimensional crowd simulation. In Chapter IV, we propose three simulation approaches to represent crowd phenomena and the integration of these methods. In Chapter V, we evaluate the proposed simulation methods through various scenarios, providing validation and analysis of the outcomes. Finally, in Chapter VI, we conclude the dissertation and discuss potential future research directions.

II. Previous Work

A. Crowd Simulation

Crowd simulation aims to reproduce and predict crowd behavior in various social situations. At a high level, crowd modeling techniques can be classified as microscopic and macroscopic models [29]. Microscopic models focus on the behavior of individual agents, while macroscopic models simulate crowds as a single entity. Macroscopic models can efficiently represent large or dense crowds, but they cannot capture the characteristics of individual agents. A representative method of macroscopic models is based on calculating the optimal velocity for each grid unit and navigating all agents within the grid [9, 10]. Microscopic models can be further classified into force-based, velocity-based, and vision-based methods. All three models aim to help agents navigate while avoiding collisions successfully. The force-based model calculates interaction forces with the surrounding environment, while the velocity-based model determines the optimal velocity by considering the velocities of neighboring agents. The vision-based model is the most human-like among the proposed methods, making decisions based on visual information gathered in various ways.

1. Force-based Model

The force-based models have been treated as synonymous with collision avoidance for a long time. The representative model of this approach is Social Force Model (SFM) [8, 35], and subsequent methods have been derived from this model [29]. SFM is a method in which agents use force to avoid collisions within crowds. These social forces typically include attractive force to reach the goal and repulsive force to avoid collisions with obstacles and other agents. The forces applied to the agents are calculated as the sum of these types of forces.

In Figure 2.1, $\vec{f}_{ij}$ and $\vec{f}_{iw}$ are repulsive forces to avoid collision with a agent j and a $wall$. $v_i^0 \vec{e}_i^0$ represents an attractive force directed toward a target. $\vec{v}_i$ is the current velocity of agent i, and $\vec{f}_i^0$ is the calculated force to be applied to the agent i. SFM is widely used due to its ease of implementation and applicability.

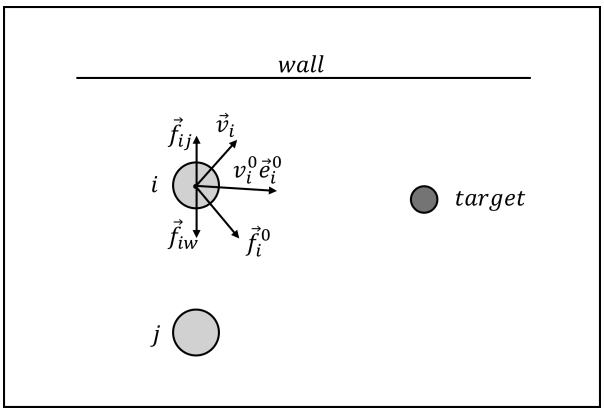

Figure 2.1. Example of SFM collision-avoidance algorithm [32]

2. Velocity-based Model

The velocity-based models involve agents navigating and avoiding collisions based on velocity values obtained from neighboring agents. A seminal work based on this method is the velocity obstacle (VO) method, where a possible collision-velocity space is considered to avoid collisions with neighboring agents [6]. VO spaces are calculated based on the velocities of neighboring agents, and to avoid collisions, the agent selects the velocity closest to the optimal velocity that lies outside the VO spaces. As an example in Figure 2.2a, the VO_{B_1} space is calculated by $\hat{B}_1$, and VO_{B_2} is calculated by $\hat{B}_2$. The agent $\hat{A}$ selects a velocity outside the regions of VO_{B_1} and VO_{B_2}.

It then evolves to reciprocal velocity obstacle (RVO) to prevent oscillations by taking into account each other's velocities [24]. Unlike VO, which did not consider the agent's own velocity,

RVO calculates the space by considering both the agent's own velocity and the velocity of the neighboring agent. As an example in Figure 2.2b, RVO is calculated by considering the velocity of agent A in addition to $VO^A_B(v_B)$.

The optimal reciprocal collision avoidance (ORCA) is a successor to RVO and is an algorithm that allows agents to analytically calculate the optimal velocity while avoiding collisions [25]. In RVO, neighboring agents generate velocity obstacles that define the velocities that would lead to collisions, represented as cone-shaped regions. In contrast, ORCA divides the velocity space into two half-planes by generating a line for each neighboring agent, allowing agents to select an optimal velocity within the collision-free space. A major difference between ORCA and RVO is that ORCA uses mathematical derivation to determine optimal velocities, making it more efficient compared to RVO.

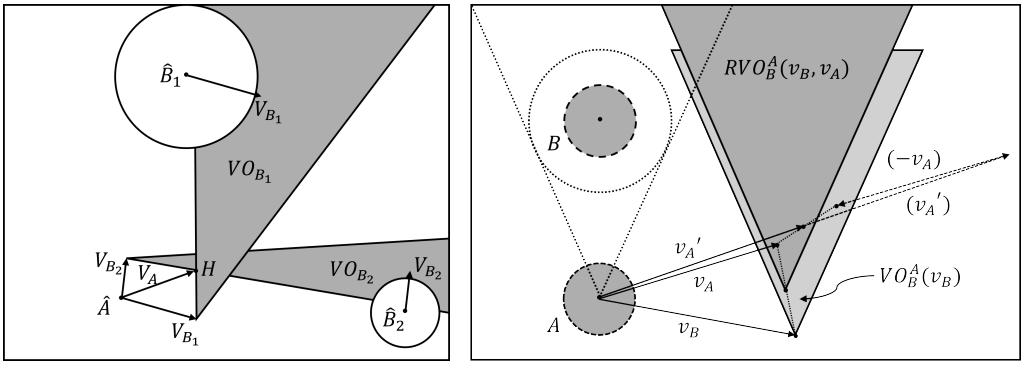

(a) VO [6] (b) RVO [24]

Figure 2.2. Example of VO (left) and RVO (right)

3. Vision-based Model

The vision-based models are derived from the fact that humans navigate using visual information. Gradient-based steering calculates costs using pixel values collected by a virtual retina of agents and finds the optimal velocity for navigation while avoiding collisions [4]. Collision risks along an agent's trajectory are minimized using a cost function. Then, partial derivatives of the cost function are computed, and agents adjust their motion by following the gradient to navigate safely.

Furthermore, methods have been proposed that calculate optical flow using differences in pixel values between consecutive frames and use this information for collision avoidance [14, 15]. Optical flow is the pattern of apparent motion of objects, surfaces, or edges in a visual scene caused by relative movements between a camera and the environment. In simulations, optical flow is used to help virtual agents perceive their surroundings by analyzing the visual data. For example, it helps agents detect obstacles, predict collisions, and adjust their paths dynamically, allowing them to navigate through complex environments in a human-like manner. Vision-based methods have the advantage of similarity to human cognitive processes, but their complexity makes them unsuitable for large-scale crowd simulations.

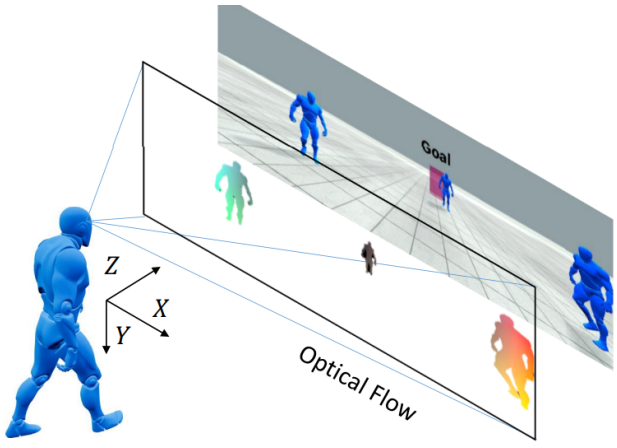

Figure 2.3. Example of the optical flow model [15]

4. Hybrid Model

Some studies integrate various simulation methods to represent high-density crowds. Van Toll *et al.* combined several microscopic methods with the fluid simulation approach, Smoothed Particle Hydrodynamics (SPH), to capture fluid-like behavior in extreme densities [26, 27]. In these studies, SPH was combined with existing crowd simulation methods, including SFM and RVO. This approach provides better stability and control at high densities while preserving individual agent behavior at lower densities. By achieving this balance, they successfully reenacted the concert scenario where crowd shockwaves occurred, as illustrated in Figure 2.4.

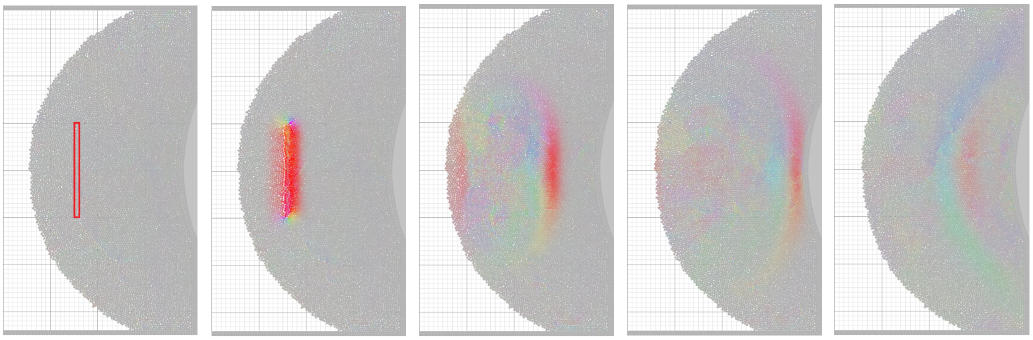

(a) t = 150s (b) t = 150.6s (c) t = 152s (d) t = 153s (e) t = 155s

Figure 2.4. Concert scenario using SPH method [26]

This dissertation uses a hybrid method to represent various crowd behaviors realistically. For low-density situations, efficient collision avoidance and navigation are necessary. While force-based models are easy to implement, they become computationally inefficient and result in unstable motion as the number of agents increases. Vision-based models require significant computation per agent, making them unsuitable for large crowds. Therefore, we use a velocity-based model, specifically RVO, for efficient collision avoidance and navigation.

To represent fluidization in high-density scenarios, we use SPH, similar to the approach by Van Toll *et al.* [26, 27]. However, we extend beyond this by employing articulated body dy-

namics to simulate crowd collapse in extreme density. This dissertation differentiates itself from previous research by transitioning between multiple simulation methods based on specific conditions and enabling their interaction.

B. Reenactment of Crowd Accidents

In the literature, there have been studies aiming to reenact actual accidents using crowd simulation. These studies aim to identify the causes of such incidents and further design preventive measures for future accidents.

1. Love Parade 2010

Studies have attempted to reenact the Love Parade disaster in Duisburg, Germany in 2010. The Love Parade is a famous music festival held in Germany, and in 2010, it took place in Duisburg. During the event, the crowd exceeded the capacity of the festival area, leading to a fatal crush. As a result, 21 people died and 342 were injured. This incident has been studied extensively due to the many aspects that can be analyzed in terms of environmental characteristics and crowd management.

Pretorius *et al.* [23] used a buildingEXODUS tool, an evacuation modeling tool working on a rule-based approach, to recreate the accident. However, the tool had limitations of representing extremely dense crowds exceeding $4P/m^2$, and it could not estimate areas prone to stampedes based solely on density. Therefore, the study added a condition where areas maintaining a density of $4P/m^2$ for more than 5 minutes were estimated as hazardous zones of stampedes. The population inflow data for the experiment was collected by analyzing CCTV footage released by the festival organizers, forming the base case. Five What-if simulations were conducted under varying conditions to suggest effective preventive measures.

Zhao *et al.* [36] utilized SFM for crowd simulation and predicted the risk of accidents based on the density map. In this study, a base scenario and nine alternative crowd management scenarios were proposed to assess the risk level in each situation. A user study was conducted to explore individuals' physiological and psychological responses to different scenarios. Participants were immersed in virtual reality (VR) simulations using head-mounted displays. Through this, the relationship between effective crowd accident countermeasures and the psychological and physical pressures experienced by the crowd was revealed.

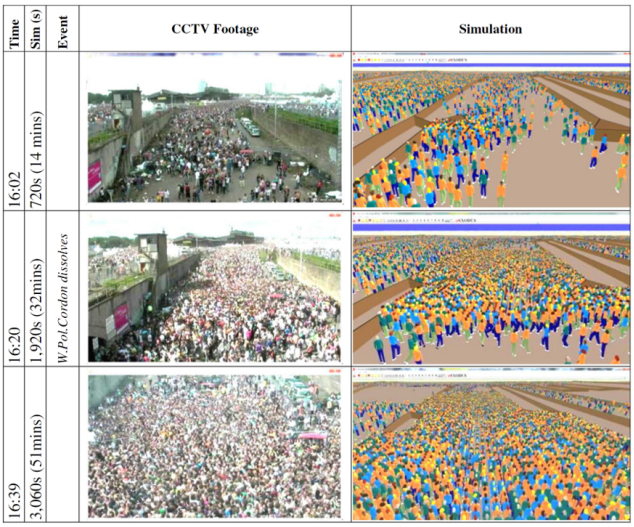

(a) Comparison of CCTV footages and simulation results [23]

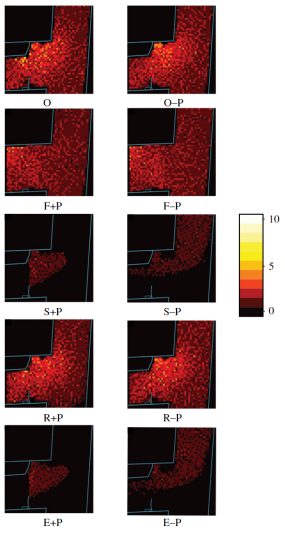

(b) Density maps of each scenario [36]

Figure 2.5. Reenactment of Love Parade 2010 crowd accidents

2. Hajj

Numerous studies have been conducted to simulate and analyze Hajj, an Islamic pilgrimage where mass crowds gather yearly, making it a high-risk event for crowd accidents. Due to the nature of Hajj being held at the same location every year, predicting and preventing crowd accidents is of utmost importance.

Mahmood *et al.* [16] proposed a framework using the Anylogic pedestrian library, a microscopic simulator to represent the complex crowd behavior of large crowds and reproduced various Hajj scenarios. In this study, various evacuation strategies for Hajj are simulated using the proposed framework, and the most effective evacuation strategy is evaluated. Furthermore, the study suggests the potential for expanding this approach to Public Safety & Security (PSS) management organizations.

Yaagoubi *et al.* [31] combined geographic information systems and microscopic modeling for simulation to reproduce Hajj and proposed plans for a safe event. Five schedules were simulated, with three involving movement from the camp entrance to the assembly area and two from the camp entrance to the Jamarat gate. Based on the pilgrim density (P/m^2) and the time required to reach the destination, the simulation results help in selecting an appropriate schedule in terms of safety and efficiency.

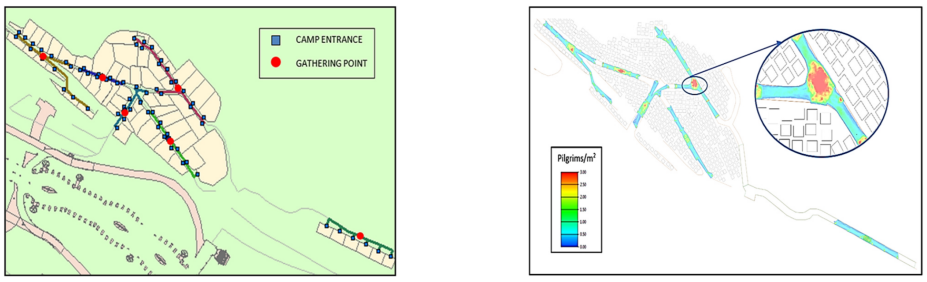

(a) Optimal routes (b) Simulation results

Figure 2.6. Example of Hajj scenario [31]

In previous studies on crowd accidents, some could not adequately represent high-density crowds, which could lead to crowd crush. Even if high-density crowds could be represented, determining whether they could lead to actual casualties was impossible, limiting their ability only to assess potential risk levels. Our proposed crowd simulation can realistically model high-density crowds and identify areas with a potential risk of leading to casualties.

III. Environment and Agents Modeling

This chapter overviews the environment and agent models for reenacting the Itaewon disaster. The models are designed to replicate the complex dynamics and crowd behaviors observed during the event. Additionally, this chapter introduces our agent transition algorithm, which enables agents to transition between different models depending on the crowd density and external conditions.

A. Environment Model Reconstruction

In order to model the disaster scene accurately, we reconstructed the Itaewon disaster site with a polygonal mesh model with textures. We use a 360-degree high-resolution RGB-D camera for scanning the environment. There are certain constraints for scanning the environment and generating 3D data. To meticulously scan the disaster area and ensure accurate data alignment, each scanning site was kept at an interval of $2m$. This distance was chosen to enhance pixel similarity, as scanned data is aligned based on its similarity to previous scans. For outdoor scanning, there is a restriction that direct sunlight should not enter, but it should be bright enough. Therefore, it was necessary to scan during the civil twilight period. To cover the accident alleys within a limited time, 37 scanning points and their sequence were chosen for scanning. We utilized the acquired three-dimensional point cloud and color data from the RGB-D camera to reconstruct the scene into a three-dimensional textured mesh model (see Figure 3.3). This model serves as an obstacle in our simulation as well as a navigable area for agents.

Figure 3.1. On-site 3D scanning of Itaewon for environment model reconstruction

Figure 3.2. Panoramic 360-degree view of the Itaewon environment

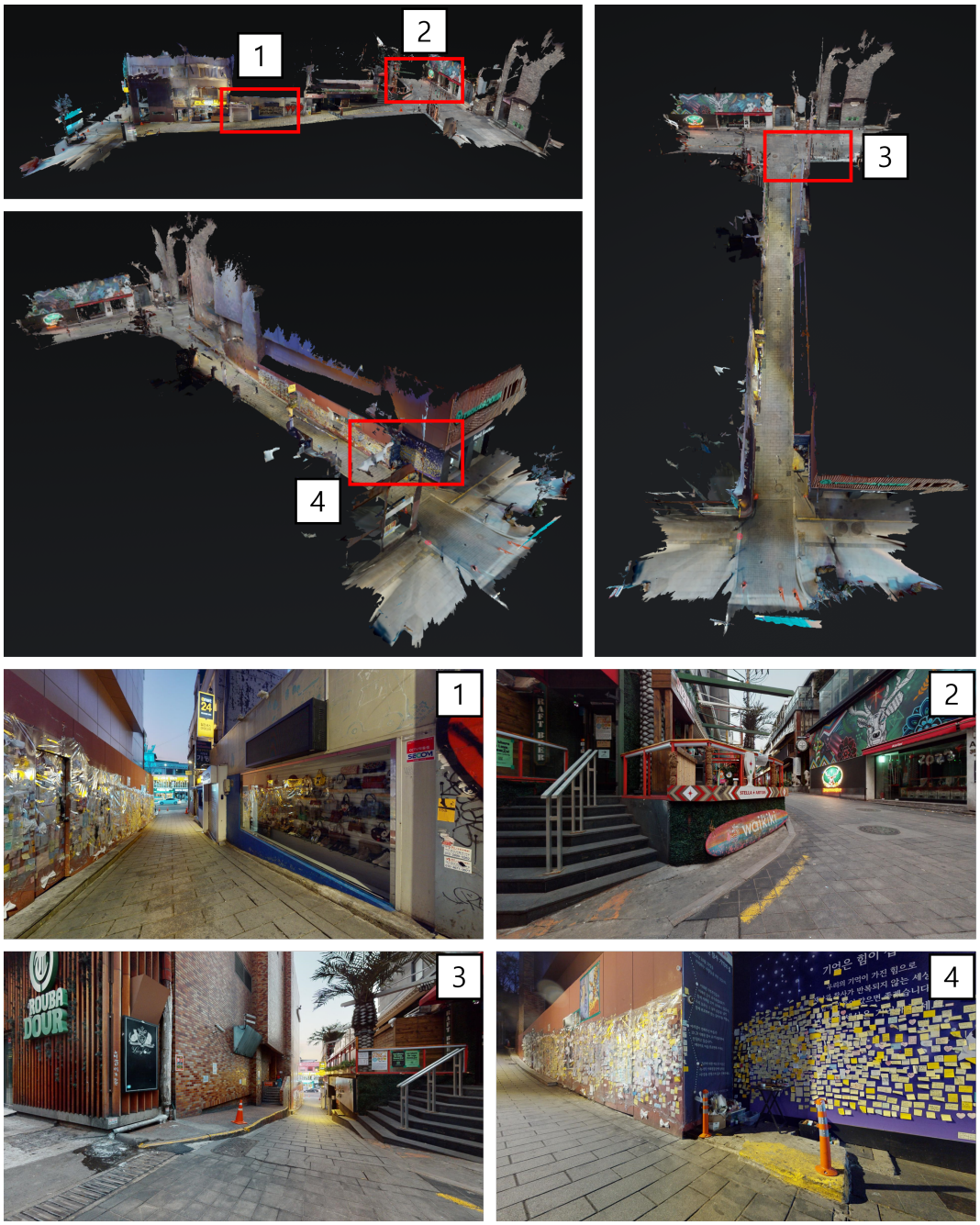

Figure 3.3. Reconstructed Itaewon 3D environment model from various views

B. Kinodynamic Agents

Crowds exhibit characteristic movements depending on their crowd density. Thus, we model the crowd $\mathcal{S}$ as a set of individual agents a_i^c with density-dependent characteristic behavior: *i.e.,* $\mathcal{S} = \{a_i^c\}$ where the characteristic behavior c in a_i^c shows either kinematic (K), hydrodynamic (H_d), hydrostatic (H_s), or articulated passive (A) behaviors, *i.e.,* $c \in \{K, H_d, H_s, A\}$. The configuration space (C-space) of each agent also depends on its characteristics in our simulation. The C-space of agents of types a^K, a^{H_d}, a^{H_s} is in SE(2) (*i.e.,* planar motion) while that of a^A is SE(3)$\times\mathrm{SO}(3)^{n_s} \times \mathbb{S}^{n_r}$ where n_s and n_r are the numbers of spherical and revolute joints in the articulated agent, respectively (*i.e.,* fully articulated motion in $\mathbb{R}^3$).

Kinematics-based crowd simulation is an efficient method for simulating collision avoidance paths among large crowds at low cost. In low-density crowds, we employ kinematics-based agents a^K where navigation while avoiding collisions is required within the Itaewon simulation. A high-density crowd resembles the movement of fluid [26] where individuals are swept along regardless of their individual will [10, 22]. At the actual Itaewon disaster scene, crowd fluidization occurred throughout the accident area. Such crowd fluidization phenomena cannot be accurately represented using only kinematic crowd simulation techniques. Therefore, we utilize the hydrodynamics simulation technique called SPH [7] to represent fluidization phenomena in high-density crowds. This type of agent is either hydrodynamic a^{H_d} or hydrostatic a^{H_s} depending on whether it is reactive (a^{H_d}) or passive (a^{H_s}). Finally, kinematic and hydrodynamic crowd simulations struggle to reproduce the chain reaction of falling, and crowd crush with high degree-of-freedom (DoF) motions observed in high-density crowds. This study addressed this limitation by incorporating articulated body dynamics with contact to accurately reproduce the falling and crowd crush phenomena witnessed in the Itaewon disaster [22, 33]. This is an a^A agent.

C. Agent Transition

This dissertation uses a mixture of simulation algorithms (*i.e.,* co-simulation) to model diverse agent behaviors. Each agent model makes transitions based on specific conditions, with density being the primary criterion, as illustrated in Figure 3.4. Therefore, we divide the navigable area of the Itaewon 3D model into uniform grids of $1m^2$ each. Kinematic, hydrodynamic, and hydrostatic agents use the density for transition. Initially, in low-density states, kinematic agents a^K are deployed. As the density of a grid reaches $\rho_h \equiv 4P/m^2$ or higher (*i.e.,* high-density crowd [26]), the agents embedded in the grid transition to hydrodynamic agents $a^K \mapsto a^{H_d}$. As the density increases to $\rho_s \equiv 12P/m^2$, which is 25% lower than the maximum crowd density observed at the actual Itaewon disaster scene [33], hydrodynamic agents no longer move toward goals and transition to hydrostatic agents or vice versa. After that, contact force rather than density is used as the criterion to transition to articulated passive agents. When the contact force of hydrostatic agents exceeds $\mathbf{f}_a \equiv 4KN$, corresponding to the estimated force exerted on the agent at the accident scene [12], they transition to articulated passive agents.

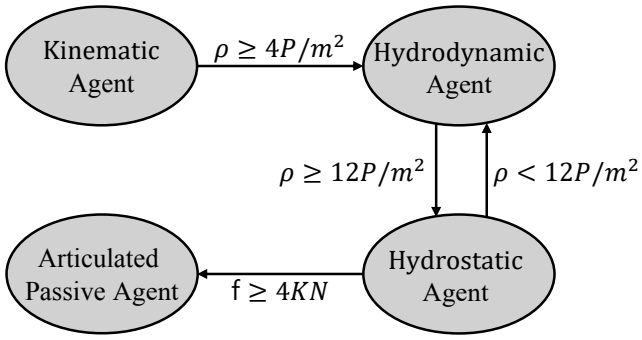

Figure 3.4. Agent transition model

IV. Extremely Dense Crowd Simulation

In this chapter, we analyze the characteristics of crowd behavior observed at the Itaewon disaster site and propose suitable simulation methods for each behavior. Additionally, we present methods for the interaction between each model.

A. Kinematic Agents

Kinematics-based crowd simulation is an efficient method for simulating collision avoidance paths among large crowds at low cost. We employ kinematics-based methods in low-density crowds where navigation while avoiding collisions is required within the Itaewon simulation. To employ such methods, in this study, we polygonize the areas with convex polygons (*i.e.,* navigation mesh) where agents can navigate within the Itaewon 3D model. The navigation mesh stores the surface as convex polygons, and polygons store information about which polygons are neighbors. Then, each agent utilizes the A* algorithm within these navigable areas to plan a global path to their destination. Agents reach their destination by moving toward the nearest corner, following a sequence of polygons generated by this algorithm. Within the alleyways of the Itaewon environment, designated as A, B for the upper left and right corners, and C, D for the lower left and right corners, respectively, we establish a total of eight global paths based on combinations of starting and ending points available to agents. In more detail, the navigation sequence is $\{A|B\} \rightarrow \{C|D\}$ or $\{C|D\} \rightarrow \{A|B\}$ (see Figure 4.1).

Additionally, to avoid collisions with other agents while moving, we employ a kinematics-based collision avoidance method such as RVO as a local collision avoidance strategy [24]. RVO defines a velocity space where collision is possible between an agent and its neighboring agents. The definition of RVO is as follows:

$$RVO_B^A(\mathbf{v}_B, \mathbf{v}_A) = \left\{ \mathbf{v}_A^{'} \mid 2\mathbf{v}_A^{'} - \mathbf{v}_A \in VO_B^A(\mathbf{v}_B) \right\} \tag{4.1}$$

$$VO_B^A(\mathbf{v}_B) = \{\mathbf{v}_A \mid \lambda(\mathbf{p}_A, \mathbf{v}_A - \mathbf{v}_B) \cap B \oplus -A \neq \emptyset\} \tag{4.2}$$

After calculating the RVOs for neighboring agents and combining them, we can find a set of collision-free velocities. Among these velocities, the one closest to the preferred velocity is selected. The maximum velocity of kinematic agents is constrained to the average walking speed of $0.6m/s$ within dense crowds [13, 30].

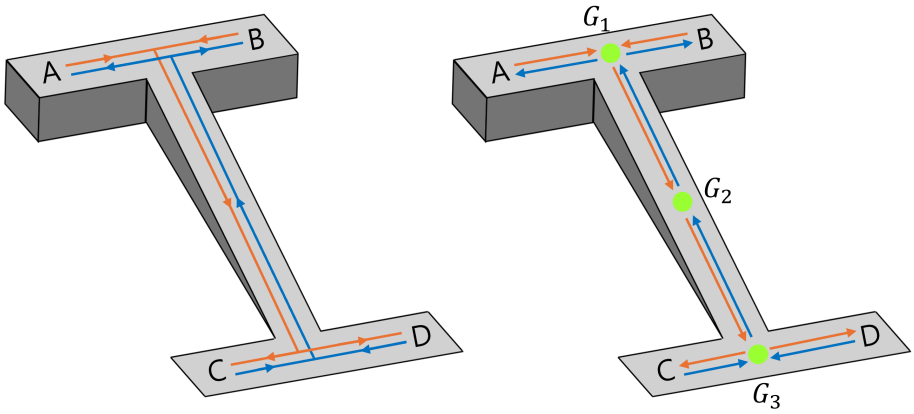

Figure 4.1. Navigational paths for kinematic agents (left) and hydrodynamic agents (right)

B. Hydrodynamic Agents

Crowds exhibit characteristic movements depending on their density. Typically, when the density exceeds $\rho \geq \rho_h \equiv 4P/m^2$, it creates a high-density crowd [26], resembling the movement of fluid where individuals are swept along regardless of their individual will [10, 22]. At the Itaewon disaster scene, a maximum crowd density of up to $16P/m^2$ was observed [33], and crowd fluidization occurred throughout the accident area. Such crowd fluidization phenomena cannot be accurately represented using kinematics-based crowd simulation techniques. Therefore, we aim to utilize the hydrodynamics simulation technique using SPH [7] to represent fluidization phenomena in high-density crowds.

In SPH, we use the function $W(\mathbf{r}, h)$, which is called the smoothing kernel with support radius h. This function adjusts the influence based on distance from $\mathbf{r}$. We can compute the density ρ and pressure p at position $\mathbf{r}$ where k is gas constant.

$$\rho(\mathbf{r}) = \sum_{j \in N(\mathbf{r})} m_j \frac{\rho(\mathbf{r}_j)}{\rho_j} W(\mathbf{r} - \mathbf{r}_j, h) = \sum_{j \in N(\mathbf{r})} m_j W(\mathbf{r} - \mathbf{r}_j, h) \tag{4.3}$$

$$p(\mathbf{r}) = k(\rho(\mathbf{r}) - \rho_0) \tag{4.4}$$

The Navier-Stockes equation formulates the conservation of momentum where $\mathbf{g}$ is an external force density field and μ is the fluid's viscosity.

$$\rho(\frac{\partial \mathbf{v}}{\partial t} + \mathbf{v} \cdot \nabla \mathbf{v}) = -\nabla p + \rho \mathbf{g} + \mu \nabla^2 \mathbf{v} \tag{4.5}$$

Then, we can get the acceleration $\mathbf{a}_i$ of agent a_i where $\mathbf{f}_i$, ρ_i, and $\mathbf{g}_i$ are the force density field, the density field, and an external force density field evaluated at the location of agent a_i, respectively, and μ is the fluid's viscosity.

$$\mathbf{a}_i = \frac{\mathbf{f}_i}{\rho_i} = \frac{-\nabla p_i + \mu \nabla^2 \mathbf{v}_i}{\rho_i} + \mathbf{g}_i. \tag{4.6}$$

We can also compute the pressure force and viscosity force using the SPH rule [7]:

$$\mathbf{f}_i^{pressure} = -\nabla p(\mathbf{r}_i) \tag{4.7}$$

$$\mathbf{f}_i^{viscosity} = \mu \nabla^2 \mathbf{v}(\mathbf{r}_i) \tag{4.8}$$

The SPH agent a_i calculates the pressure and viscosity in Equation 4.7 and Equation 4.8 of neighboring agents and finally computes the $\mathbf{a}_i$ in Equation 4.6. The computed $\mathbf{a}_i$ is then used to calculate the velocity and position of a_i based on time integration.

We classified the SPH agent model into two categories, hydrodynamic and hydrostatic agents, based on the density field ρ. For densities of $\rho < \rho_s \equiv 12P/m^2$, agents exhibit hydrodynamic movements while showing the intention to move to their destination by setting the external force density field $\mathbf{g}_i$ to the goal-reaching force. For densities exceeding $\rho \geq \rho_s$, the ability to move to the destination is completely lost, and the simulation is static or hydrostatic by setting $\mathbf{g}_i = 0$. Hydrodynamic agents navigate using three sub-goal positions (see Fig. 4.1). Agents departing from points A and B navigate towards sub-goals G_1, G_2, and G_3 in the sequence. Conversely, agents departing from points C and D navigate reversely, following sub-goals G_3, G_2, and G_1. In short, there are three sub-goal positions starting from $\{A, B, C, D\}$, and the navigation sequence is $\{A|B\} \rightarrow G_1 \rightarrow G_2 \rightarrow G_3$ or $\{C|D\} \rightarrow G_3 \rightarrow G_2 \rightarrow G_1$, as illustrated in Figure 4.1. The goal-reaching force is then defined as follows:

$$\mathbf{g}_i = \mathbf{f}_i^{goal} = k^{goal} \frac{(\mathbf{r}_{goal} - \mathbf{r}_i)}{\|(\mathbf{r}_{goal} - \mathbf{r}_i)\|}, \tag{4.9}$$

where k^{goal} is a force gain and $\mathbf{r}_{goal}$ is the position of one of the sub-goals $\{G_1|G_2|G_3\}$

To properly set the density threshold ρ_s for transition, we divided the navigable area of the Itaewon model into grids of $1m^2$ each. Moreover, as the kinematic agent switches to the hydrodynamic agent when the crowd density reaches ρ_h, the walking speed of the crowd no longer decreases but maintains a speed of $0.4m/s$ [13]. Therefore, we count the number of agents within each grid area whose walking speed is less than $0.4m/s$. The number of agents within such grids is used as the density of the grid.

C. Articulated Passive Agents

Based on the observation of falling occurrences within extreme-density crowds where fluid-like behavior emerges, we model agents behaving according to fluid dynamics to have fallen when subjected to forces exceeding $\mathbf{f}_a \equiv 4KN$. Subsequently, articulated body dynamics were applied, allowing agents to respond passively to external forces, including collision reactions, once they fell.

A typical formulation that governs articulated body dynamics can be defined as a pair of rigid bodies connected by a joint in generalized coordinate θ [19]:

$$\mathbf{M}(\theta)\ddot{\theta} + \mathbf{C}(\theta, \dot{\theta})\dot{\theta} + \mathbf{N}(\theta, \dot{\theta}) = 0, \tag{4.10}$$

where $\mathbf{M}, \mathbf{C}, \mathbf{N}$ represent the inertia matrix, the Coriolis matrix, and external forces, respectively. The agents' physical attributes reflect average adult male and female heights and weights, setting male agents at $175cm$ and $70kg$ and female agents at $160cm$ and $56kg$. Each agent has eleven rigid bodies with six spherical joints and four revolute joints - 22 DoFs in total. Additionally, we color-coded the agent due to the contact forces resulting from crowd interactions using heatmaps, offering a visualization of the forces experienced by each agent, as shown in Figure 4.2d.

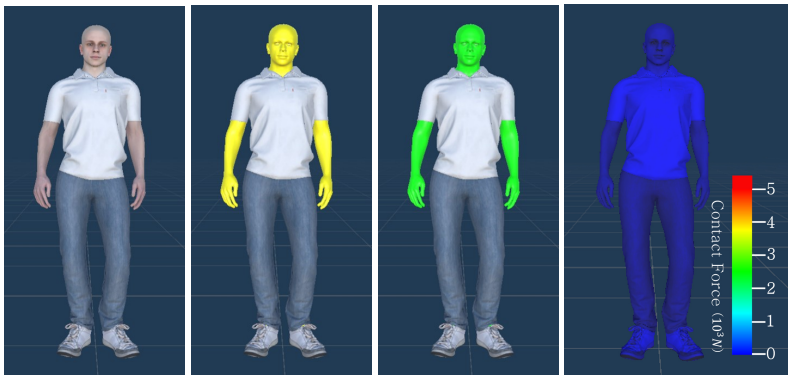

(a) Kinematic (b) Hydrodynamic (c) Hydrostatic (d) Articulated Passive

Figure 4.2. Kinodynamic agents

D. Co-simulation of Agents

Since we use co-simulation of agents in this dissertation, designing an interface for interaction among these agents is necessary. Overall, each agent must share mass, velocity, density, and pressure values with other agents for interaction. In our work, this information sharing is performed via message passing among agents.

1. Kinematic agents a_i^K need the *kinematic information*, such as the positions $\mathbf{p}_j$ and velocities $\mathbf{v}_j$, of other agents $\{a_j | \forall j \neq i\}$ or obstacles, mainly for collision avoidance. Therefore, these agents need to receive the state information not only from other kinematic agents but also from all hydrodynamic, hydrostatic and articulated passive agents to avoid collisions.

2. Hydrodynamic and hydrostatic agents $a_i^{H_d}$ and $a_i^{H_s}$ must know other agents' positions $\mathbf{p}_j$, pressure p_j, and density ρ_j. Therefore, regardless of their simulation types, all agents $\{a_j | \forall j\}$ need to contribute to calculating *dynamic information* such as pressure and density and share these values with hydrodynamic and hydrostatic agents.

3. Articulated passive agents a_i^A move by gravity or contact forces exerted by other agents that act like rigid obstacles. Therefore, they must receive *kinematic information* from other agents $\{a_j | \forall j \neq i\}$.

In our implementation, the interaction among agents is performed only for nearby agents within some distance. We employ KD-Tree as the underlying proximity data structure to do so efficiently. KD-Tree is a type of binary tree that partitions space into a hierarchical structure of points, allowing for fast search operations. Each agent finds its neighboring agents stored in the KD-Tree at the beginning of the simulation loop and then performs calculations based on the properties of those agents.

V. Results and Discussions

In this chapter, we provide a detailed explanation of the implementation of our crowd model and evaluate the simulation results. For evaluation, we compared Itaewon CCTV footage, analyzed crowd crush behaviors, performed an ablation study, simulated What-if scenarios, and replicated two other real-world crowd accidents.

A. Implementation Details

We scan and reconstruct the Itaewon environment model using the Matterport Pro2 RGB-D camera. The Matterport Pro2 Camera is a high-resolution RGB-D camera with a 360-degree left-right rotation and a 300-degree vertical field of view. Point cloud information is collected through scanning, and a 3D mesh of the model is built from the point cloud. The environment was scanned at 37 sites during civil twilight before the sun rose for 50 minutes to resemble a similar illuminance to the Itaewon disaster, and very few pedestrians were present at the scene to scan only the environment. The reconstructed Itaewon environment model consists of $360K$ triangles.

We implement the kinematic and the articulated passive agents using the navigation and the ragdoll systems, respectively, in Unity 3D engine. We use the Unity editor version of 2022.3.34f1. We also implement the hydrodynamic agents based on UMANS [28], an open-source framework for crowd simulation. Simulations ran on an Intel Core i9 processor, 32GB of RAM, and NVIDIA GeForce RTX 3090 Ti.

The simulation used $6K$ agents, and $5K$ frames were recorded at a speed of 24 simulation frames per second. The agent spawn locations and destinations were specified for each scenario, and agents were generated at chosen time intervals.

B. Parameter Settings

The detailed values used for agents in our experiment are as follows:

- The maximum speed of kinematic, hydrodynamic and hydrostatic agents is $0.6m/s$, and the maximum acceleration is $5.0m/s^2$.
- For SPH variables, the kernel support radius h is $1m$, and the rest density ρ_0 is $4P/m^2$.
- For SPH constants, the gas constant k is 100, and the viscosity μ is 1.

As shown in Figure 5.1, agents are composed of 11 body parts, with characteristics described in Table 5.1.

Table 5.1. Agent properties

	Man	Woman
DoFs	22	22
Height(cm)	175	160
Weight(kg)	70	65

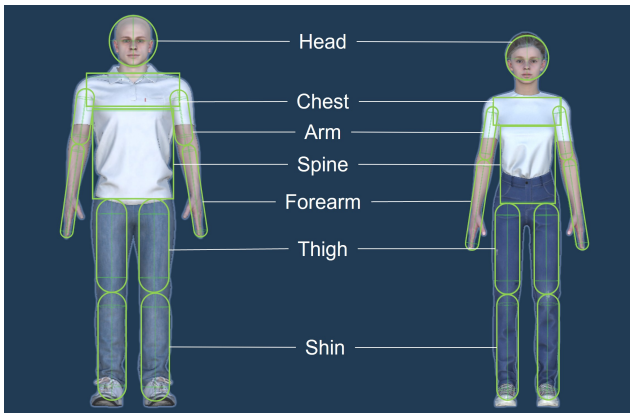

Figure 5.1. Agent model used in our system

The parameters for the three scenes used in the experiments are described in Table 5.2.

Table 5.2. Scene configuration parameters

	Itaewon	Love Parade	Oasis Concert
Scene area size	540	576	4624
# of agents generated per second	42	45	100
Total # of agents	6000	6000	6000

C. Evaluation

In order to evaluate the authenticity and plausibility of our simulation methods, we conducted five main experiments.

1. We compare our simulation results with the Itaewon CCTV footage recorded during the accident, particularly crowd fluidization.
2. We highlight the crowd crush behavior simulated using our method, showing stampedes and the domino effect of the crowd falling.
3. We perform an ablation study to highlight the contribution of different agent types to simulating high-density crowds.
4. We conduct three What-if scenarios using our crowd simulation techniques to illustrate the potential of our simulation in predicting crowd behavior and supporting future accident prevention efforts.
5. We model and simulate two other real-world crowd accidents to showcase the applicability of our crowd simulation methodology.

1. Overview of Itaewon Crowd Simulation

Before analyzing the results of each experiment in detail, we provide an overview of the general progression of the Itaewon simulation. Figure 5.2(a) shows kinematic agents navigating toward their goals from the four entrances of Itaewon. Agents generated at positions A and B move toward Itaewon Station, while those from positions C and D head toward World Food Culture Street. Initially, when the density is low, these agents are represented as kinematic agents.

As they gradually gather in the accident alley, the crowd density increases, making navigation difficult and leading to fluidization. As illustrated in Figure 5.2(b), the agents transition to hydrodynamic agents under these conditions. Figure 5.2(c) shows that as newly generated kinematic agents continue to push them, these hydrodynamic agents transition to hydrostatic agents at extreme densities where movement becomes nearly impossible.

At bottleneck areas like the T-junction, agents experience significant forces, leading to their transition to articulated passive agents. These agents, with color-coded body parts, represent the crowd collapse, as shown in Figure 5.2(d).

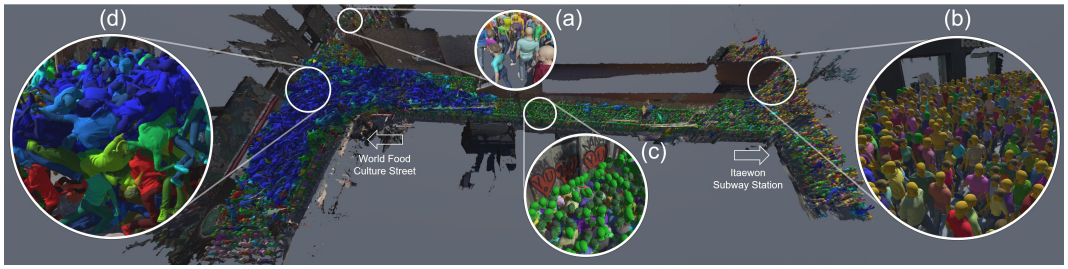

Figure 5.2. Overview of Itaewon crowd crush simulation

2. Comparison with Itaewon CCTV

The Itaewon disaster special investigation headquarters released two CCTV footage (CCTV 4-1 and CCTV 5-2) depicting the scene before and after the crowd crush [5]. We analyze these two CCTV footage and compare them with the simulation results.

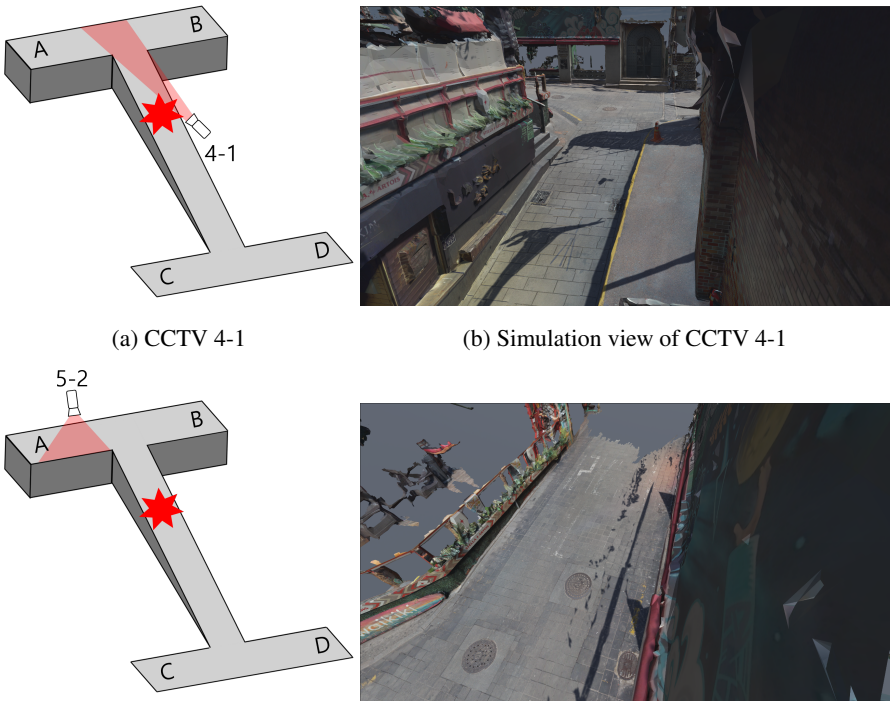

(a) CCTV 4-1 (b) Simulation view of CCTV 4-1

(c) CCTV 5-2 (d) Simulation view of CCTV 5-2

Figure 5.3. The location of CCTV and the virtual camera views

The high crowd density and blur in the CCTV footage posed challenges in tracking the motion of individuals. Therefore, we used the Computer Vision Annotation Tool (CVAT) [17] to track individuals with distinguishable features semi-automatically. Virtual cameras were positioned in the simulation scene to capture perspectives similar to the CCTV footage (see Figure 5.3). From this footage, we could observe three main types of crowd behavior:

- Type 1: moving toward the accident alley,
- Type 2: moving away from the accident alley,
- Type 3: hovering in place.

We analyze such behaviors from the CCTV footage and compare our simulation results where the simulated agents are positioned in locations similar to those selected during CCTV tracking.

CCTV 4-1 What should be noted is the change in the direction of crowd movement and fluidization according to the increase in density. Firstly, in the case of crowd movement, it is possible to move in both directions at first (the first and second column in Figure 5.4), but from just before the accident (the third column in Figure 5.4), it is possible to move only in the direction down the slope. In the alley shown in CCTV 4-1, despite the high density making it difficult for people to move, the population continues to flow in. Eventually, this leads to fluidization, with people rapidly pushed down (the third and fourth columns in Figure 5.4). The simulation results demonstrated a similarity in crowd movement direction changes to what actually occurred. In a more detailed breakdown:

1. Five minutes before the accident (Figure 5.4a), most of the crowd exhibited Type 1 behavior, but Type 2 behavior was also observed on the right side of the alley. Similarly, in the simulation results (Figure 5.4b), initially, most agents exhibit Type 1 behavior, moving downward the alley. However, some agents display Type 2 behavior, oscillating between hydrodynamic and hydrostatic agents as they move upward the alley.

2. Two minutes before the accident (Figure 5.4c), Type 1 and Type 2 behaviors were still observed. However, due to increased density, individuals behaving as Type 2 could not proceed further and transitioned to Type 3. This transition was also observed in the simulation results (Figure 5.4d), where the agents oscillating between the hydrodynamic and hydrostatic transition to hydrostatic agents, individuals behaving as Type 2 transitioned to Type 3. As the density increases, the force experienced by the agents also increases, leading to the emergence of articulated passive agents, which is hard to observe from the blurred footage.

3. Just before the accident (Figure 5.4e), Type 2 behavior was no longer observed. Strong Type 1 flow was observed on the left side of the alley, while on the right side, individuals almost stopped and exhibited Type 3 behavior. In the simulation results (Figure 5.4f), Type 2 behavior was also not observed, and differences in flow were observed between the left and right sides. The flow from the left side of the alley is faster than the flow from the right side. This difference in the flow of CCTV footage and simulation results is attributed to the bottleneck shape of the alley, which skews to the left.

4. After the accident (Figure 5.4g), Type 1 and Type 3 behaviors were observed in the footage. However, in simulation results (Figure 5.4h), only Type 1 behavior was shown, and some agents at the top of the alley transitioned to articulated passive agents.

(a) 5 min before the accident

(b) 1440 frame

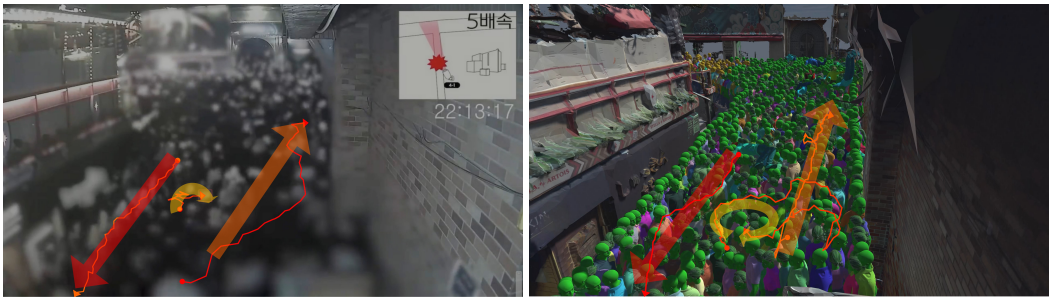

(c) 2 min before the accident

(d) 1920 frame

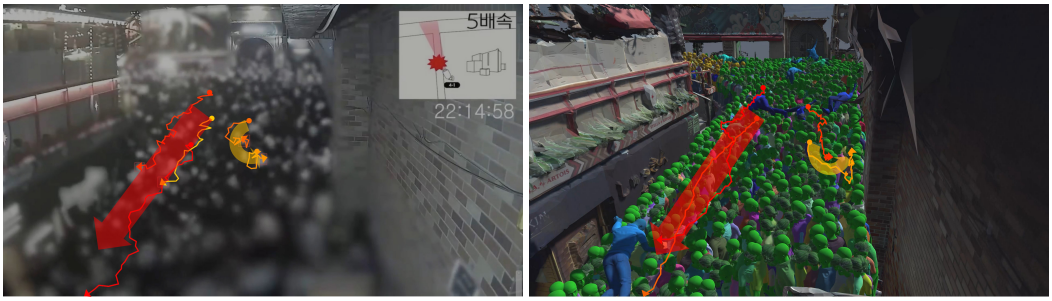

(e) Just before the accident

(f) 1920 frame

(g) After the accident

(h) 2400 frame

Figure 5.4. Video footage of CCTV 4-1 (left) vs. our simulation (right)

CCTV 5-2 The notable point is the fluidization phenomenon where as more people continued to enter the alley, they started to move rapidly, exhibiting a fluid-like behavior (Figure 5.5c-Figure 5.5g). The simulation results show the fluidization phenomenon of the crowd continuously flowing into the accident alley (Figure 5.5b-Figure 5.5h). In a more detailed breakdown:

1. Four minutes before the accident (Figure 5.5a), most of the crowds exhibited Type 3 behavior, where they hardly moved. However, in the simulation results (Figure 5.5b), most agents transitioned to hydrodynamic agents, behaving like fluid and showing Type 1 behavior and the kinematic agents entering the alley push and move the hydrodynamic agents.

2. Three minutes before the accident (Figure 5.5c), most of the crowd remains in a state of Type 3, but a few individuals exhibit Type 1 behavior, moving rapidly towards the alley. In the simulation results (Figure 5.5d), similar to the previous findings, most agents demonstrate Type 1 behavior, and as the density increases near the accident alley, agents transition into hydrostatic agents.

3. Two minutes before the accident (Figure 5.5e), Type 3 behavior, where individuals remain stationary, is no longer observed. Most of the crowd demonstrates Type 1 behavior, rapidly moving towards the accident alley. The simulation results (Figure 5.5f) also reflect this Type 1 behavior.

4. After the accident (Figure 5.5g), there was no improvement in crowd density, and Type 1 behavior, similar to the situation before the accident, is observed in both the actual and simulated results (Figure 5.5h). Furthermore, there is a continuous influx of agents into the alley, increasing the proportion of hydrostatic agents near the accident alley, and the articulated passive agents appear.

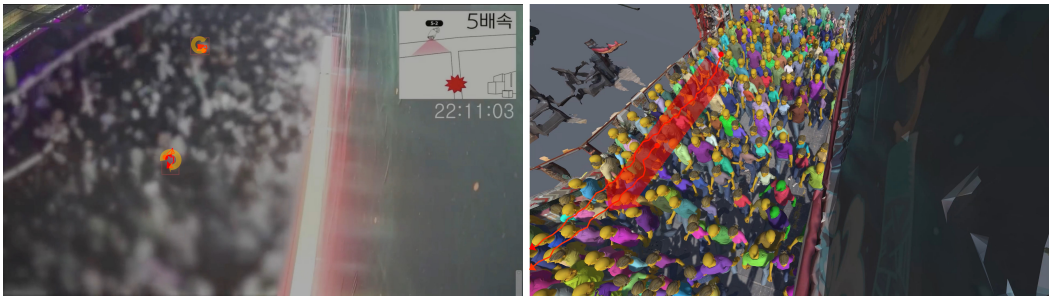

(a) 4 min before the accident

(b) 2160 frame

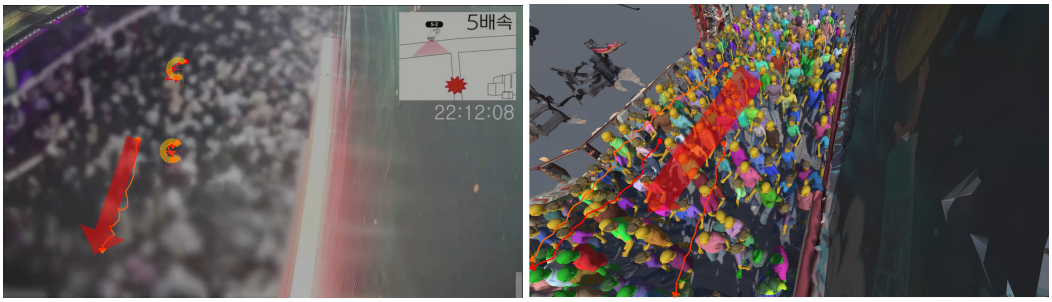

(c) 3 min before the accident

(d) 2640 frame

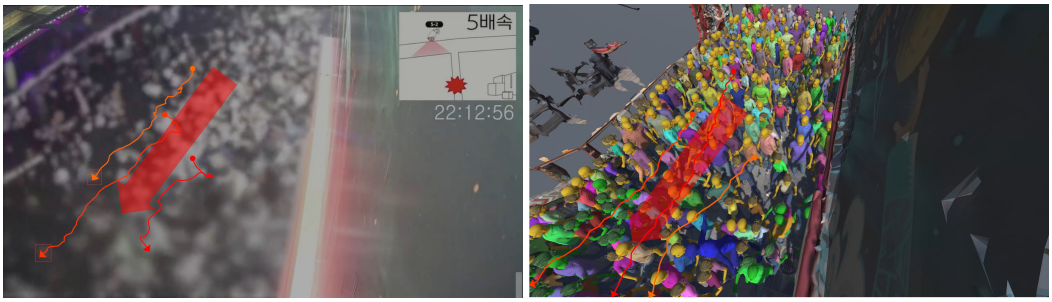

(e) 2 min before the accident

(f) 2880 frame

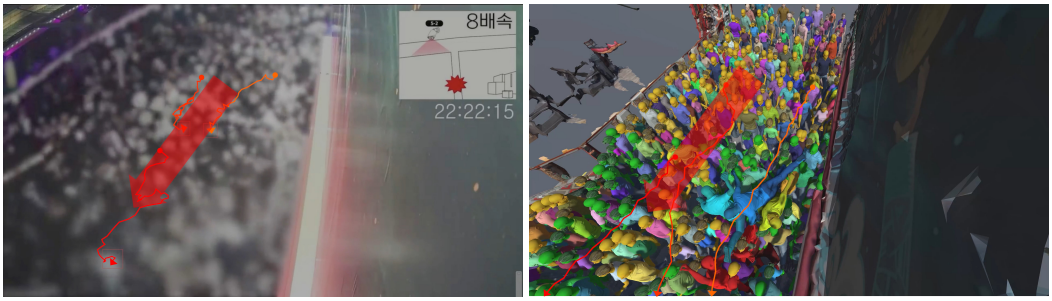

(g) After the accident

(h) 3600 frame

Figure 5.5. Video footage of CCTV 5-2 (left) vs. our simulation (right)

3. Crowd Crush Behaviors

Most casualties occurred in the narrow alley right below CCTV 4-1 due to crowd crush, whose video footage is unavailable. Hence, we use our simulation results to estimate the areas where the articulated passive (AP) agents are dominantly employed to simulate the crowd crush. Starting from Figure 5.6a, AP agents color-coded as in Figure 4.2d appear at the T-shaped entryway and gradually spread, causing the agents at the upper part of the alley to transition into AP agents overall. The area where the transition to AP agents occurs includes regions where actual casualties occurred. This indicates that AP agents can accurately represent agents in particularly hazardous conditions. During the simulation, the maximum force experienced by AP agents is $4KN$ on average, which is close to an expert estimate [12]. Through the hybrid agents we propose, we can also reproduce crowd falling and the domino effect. To verify the domino effect, we continued the simulation even after a sufficient number of agents had transitioned to AP agents. Starting from Figure 5.6d, numerous agents at the bottom left of the alley experienced significant force and transitioned to AP agents, colored red. We observed a domino effect where agents continuously toppled over, propagating the effect upward, causing overall agents in the alley to fall. As in the real incident, the domino effect occurred in the middle of the alley [22, 33].

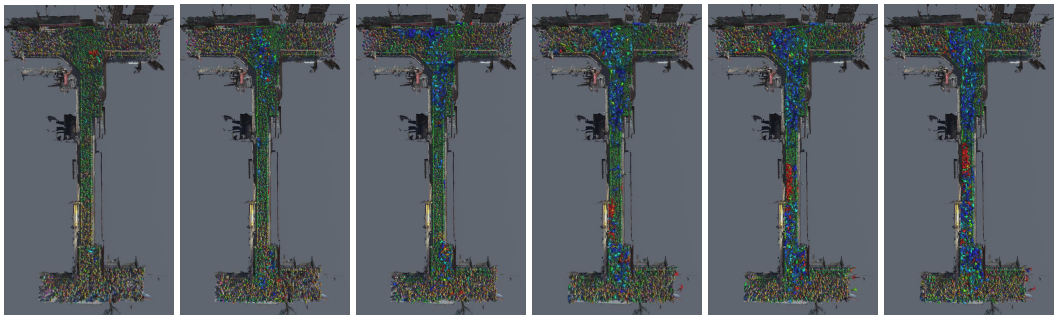

(a) 90s (b) 120s (c) 150s (d) 176s (e) 180s (f) 184s

Figure 5.6. Crowd crush simulation results from a top view

4. Ablation Study

We compared different combinations of kinematic, hydrodynamic, and hydrostatic agents to assess the contribution of each agent type to crowd density. We exclude the articulated passive agents from this ablation study as they do not directly contribute to elevating the crowd density. When using only kinematic agents (Figure 5.7a, Figure 5.7b), even after generating a sufficient number of agents, the density at the accident point does not reach $16P/m^2$, failing to reproduce the overall high-density crowd state. When using only hydrodynamic and hydrostatic agents (Figure 5.7c, Figure 5.7d), while the high-density crowd state can be reproduced, it is formed only locally. Notably, the density does not increase significantly below the T-junction entry point, with the highest number of casualties. However, when kinematic, hydrodynamic and hydrostatic agents are used (Figure 5.7e, Figure 5.7f), it can accurately represent a high-density condition overall, including below the T-junction entrance.

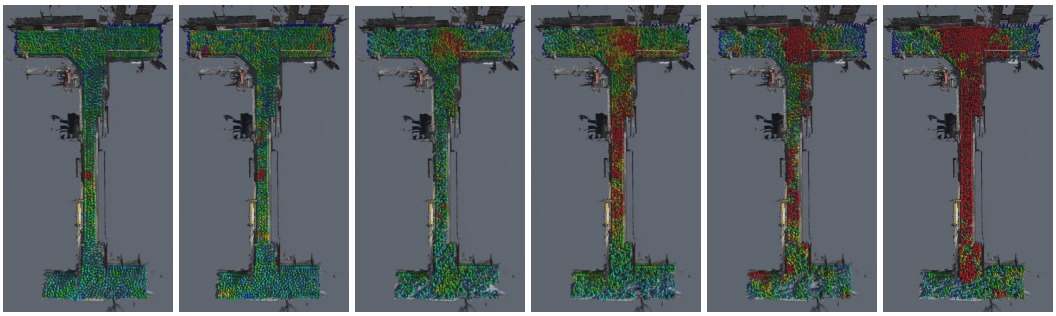

(a) K (b) K (c) $H_{d,s}$ (d) $H_{d,s}$ (e) $K + H_{d,s}$ (f) $K + H_{d,s}$

Figure 5.7. Ablation results from a top view

5. Simulating What-if Scenarios

We conduct three what-if scenarios, as suggested by disaster management experts, to assess the potential of our crowd simulation techniques in preventing incidents like the Itaewon disaster. Experts identify three main causes of the disaster: the failure to control crowd flow, an overwhelming influx of people exceeding the space's capacity, and the failure to maintain the minimum road width due to illegal structures in the narrow alley [2]. Therefore, we set up what-if scenarios for implementing right-hand traffic (RHT), controlling the influx of people (CI), and removing extensions (RE), and then run our simulation to observe their effects.

- Removing extensions (Figure 5.8b): we expand the walkable alley by deleting the building extensions from the model. The simulation results show a reduction in crowd density in the areas where the extensions are removed, but there is little change in the density at the accident site.
- Enforcing right-hand traffic (Figure 5.8c): we divide the navigable area for our RVO agents into two halves, forcing the agents to move only in the right direction based on their position. The results show that RHT alleviates overall crowd congestion, especially in the bottom alley. However, in the upper alley, where the population exceeds capacity, the right-hand traffic rule does not ease the flow.
- Controlling the influx of people (Figure 5.8d): we limit the number of agents to the maximum capacity based on the area of the Itaewon 3D model, which is 540m², with a maximum density of $4P/m^2$, capping the total at 2,160 agents. Additionally, following the experts' suggestion to have subway trains bypass Itaewon Station, agents are not generated from the bottom right alley. Simulation results show that while a high-density state still occurs in the central alley, the density in both the upper and bottom alleys is significantly reduced.
- All combined (Figure 5.8e): we conduct a simulation by combining all of the scenarios above (RE, RHT, and CI scenarios). The simulation results show that, aside from brief

disruptions near the T-junction, the overall crowd flow became smoother, and the crowd density was maintained at a reasonable level.

Through these what-if experiments, we can conclude that the accident prevention measures proposed by experts were indeed effective in mitigating the situation; in particular, combining all three suggestive measures is much more effective. Additionally, our simulation method demonstrates its potential for developing safety management strategies at large crowd-gathering events and preventing future accidents.

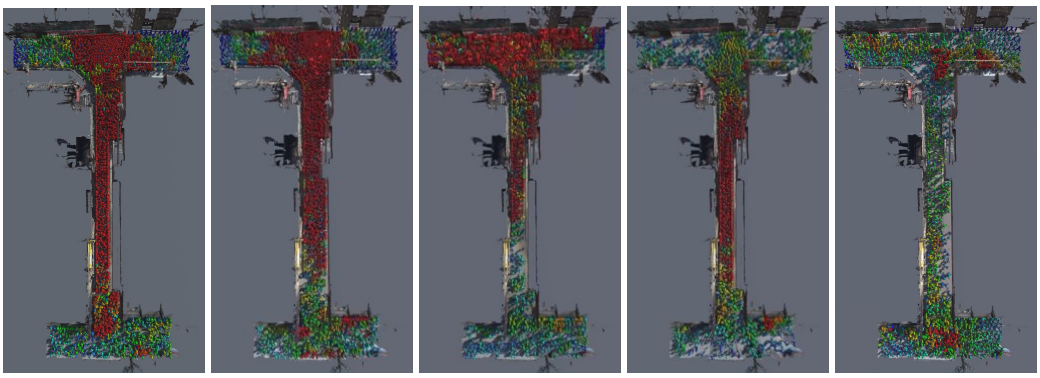

(a) BaseLine (b) RE (c) RHT (d) CI (e) Mix

Figure 5.8. What-if scenario results from a top view

6. Simulating Other Crowd Accidents

To verify the applicability of our simulation to different environments, we selected and reenacted two other real-world crowd accidents.

Love Parade 2010 The Love Parade was a renowned music festival that attracted large crowds annually. In 2010, the festival was held in Duisburg, where inadequate event space led to a crowd disaster, resulting in 21 fatalities. This accident has been extensively analyzed due to environmental structure and crowd management factors. We use $6K$ agents, the same as in the previous Itaewon scenario, and employ a virtual environment with half the width of the actual site to match the number of agents. Agents are generated at three locations: A, B, and C, as illustrated in Figure 5.9a. Agents generated at A move toward the exit at B, while those generated at B and C head toward A.

In Figure 5.9a, the areas marked in red indicate regions where casualties were concentrated at the actual accident site. This area is a T-junction where crowds converge from both sides, and the alley where the crowd gathers is wider than the ends of the T-junction. The organizers of the Love Parade released recordings from a total of seven CCTV cameras, among which camera 13 covered the accident area. Therefore, we tracked and compared the movement patterns in the CCTV footage with our simulation results. As shown in Figure 5.9b, the crowd in the CCTV footage remains in place, and when the balance is disrupted, they exhibit a surge characteristic of crowd fluidization. Similarly, in the simulation results, the agents stay in position, displaying brief flows caused by the crowd fluidization effect.

To further validate the accuracy of our simulation, we assessed whether high-risk areas were estimated. As shown in Figure 5.9c to Figure 5.9f, the overall density of the given area increases, leading to the emergence of hydrodynamic and hydrostatic agents. Notably, similar to the actual accident site, the density rises more rapidly in area A, which has a broader space, compared to the narrower areas B and C. Consequently, articulated passive agents also appear in locations

similar to where casualties were concentrated in the actual incident.

Through the Love Parade scenario, we verify that our simulation can also be applied in different environments, effectively capturing crowd fluidization and estimating high-risk areas.

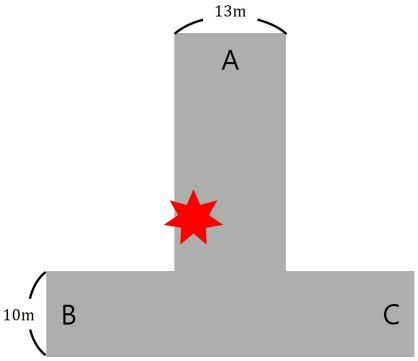

(a) Love Parade configuration

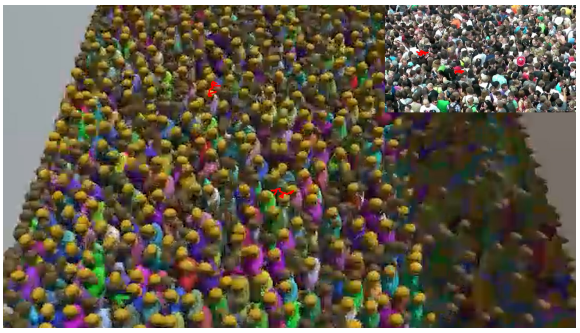

(b) Comparison with video footage

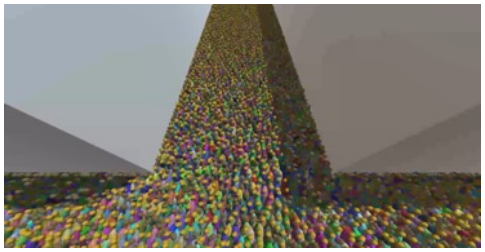

(c) 110s

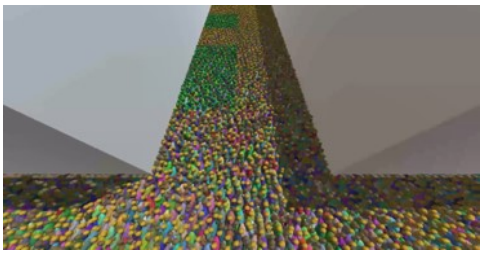

(d) 120s

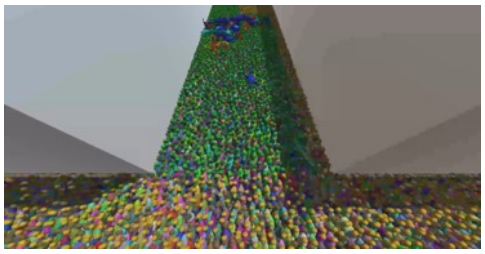

(e) 130s

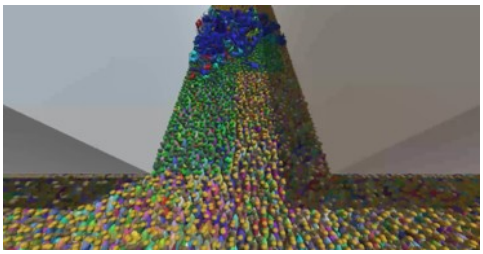

(f) 140s

Figure 5.9. Love Parade 2010 configuration and results from a top view

Oasis Concert 2005 The Oasis Concert accident was caused by an excessive number of people crowding the concert floor. Although the concert was stopped before the situation escalated, preventing fatalities, wave surges were clearly visible, making it a frequently studied case for high-density crowd experiments. In Figure 5.11a, the orange lines indicate the locations where agents are generated, with $6K$ agents being created. Each agent is randomly assigned a goal force between 5 and 10 and moves towards the goals represented by a green circle.

As shown in Figures 5.11b to 5.11f, the generated agents move towards the center of the stage. At this point, the moving crowd can be divided into areas with sparse and dense density. In the sparse areas, kinematic agents appear, and some of them deviate from the shortest path and take a detour depending on the crowd density. In the dense areas, hydrodynamic agents emerge, navigating directly toward the center of the stage.

To observe the crowd wave effect, we selected 60 agents and applied a strong force to push them toward the stage. We also applied color coding based on agents' velocity to visualize the wave's propagation. Then, we compared the wave phenomenon with footage from the concert. As seen in Figure 5.10, the crowd wave that starts from the back is transmitted forward in both the footage and the simulation results. From Figure 5.11g to Figure 5.11n, we can see that the crowd wave, initially propagating toward the stage, collides with the stage and reverses direction, spreading back toward the rear.

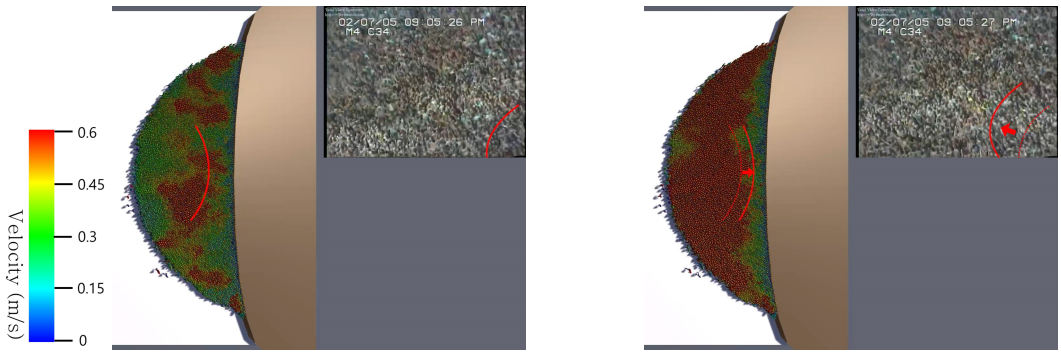

(a) (b)

Figure 5.10. Detailed view of crowd surge propagation

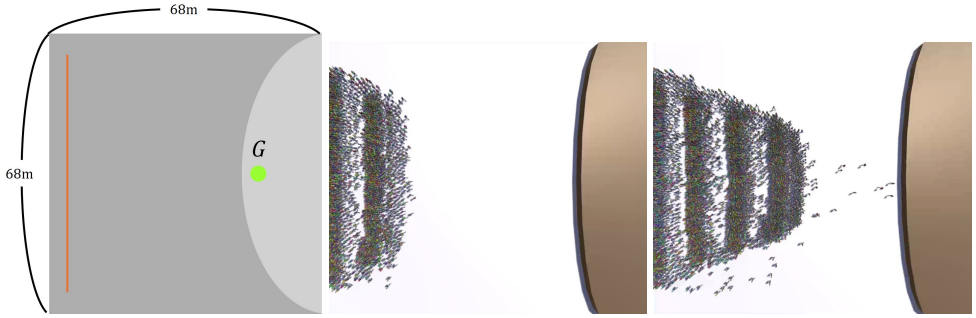

(a) Oasis Concert configuration (b) 20s (c) 40s

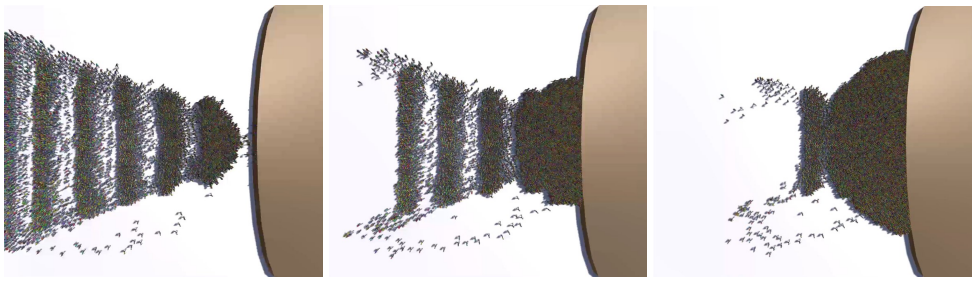

(d) 60s (e) 80s (f) 100s

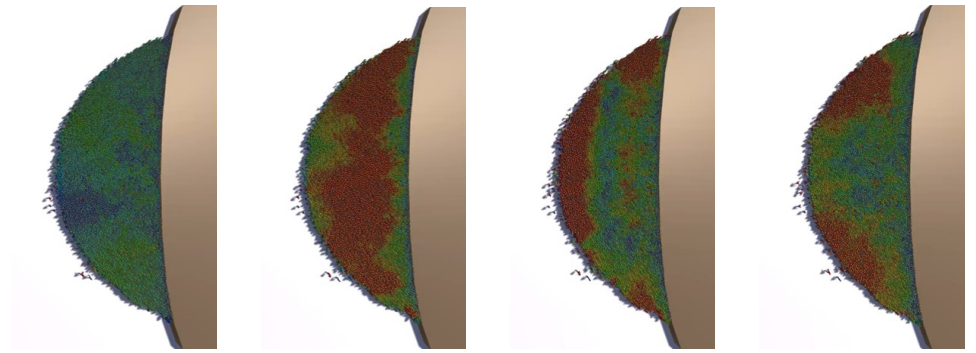

(g) 151s (h) 151.5s (i) 152s (j) 152.3s

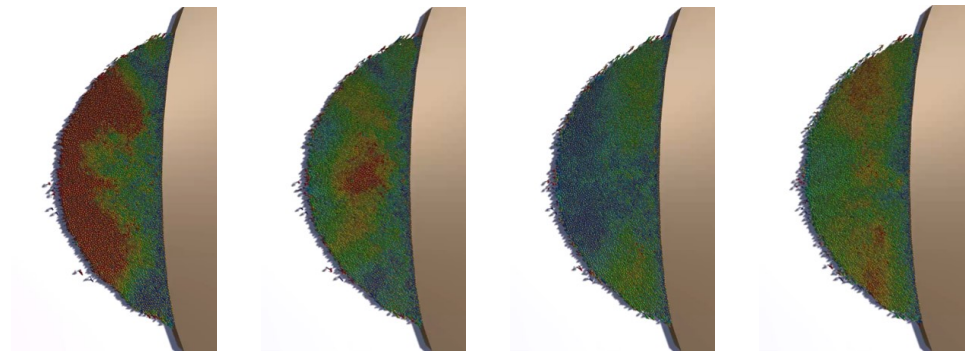

(k) 152.7s (l) 153s (m) 153.3s (n) 153.7s

Figure 5.11. Oasis Concert 2005 configuration and results from a top view

VI. Conclusion

This dissertation proposes a co-simulation of kinodynamic agents via message passing and shared data structures to reproduce the Itaewon crowd crush. We conducted experiments to verify that our kinodynamic agents can demonstrate fluidization, crowd collapses, and domino effects occurring in high-density crowds, with their behaviors compared to the actual Itaewon CCTV footage.

The simulation results show that our approach can accurately represent different crowd dynamics, including the transition from kinematic to hydrodynamic and hydrostatic behaviors under varying density conditions. We also demonstrated the effectiveness of the articulated passive agent model in representing crowd collapses at critical areas, such as the T-junction in the Itaewon disaster, where casualties were concentrated.

Furthermore, through the ablation study, we highlighted the contributions of different agent types, including kinematic, hydrodynamic, hydrostatic, and articulated passive agents, in enhancing the accuracy of the simulation under different density levels. This study also illustrates the advantages of using a hybrid simulation approach that combines multiple agent behaviors to capture complex phenomena observed in real-world crowd incidents.

The three what-if scenarios conducted as part of our experiments, such as controlling the influx of people, enforcing right-hand traffic, and removing illegal structures, demonstrate the potential of our simulation to be used as a decision-making tool for urban planners and safety authorities. These scenarios provided insights into how different intervention strategies can effectively reduce crowd density and prevent catastrophic outcomes during large public gatherings.

To verify the applicability and adaptability of our simulation methods, we successfully reproduced two additional real-world crowd accidents: the Love Parade disaster and the Oasis Concert crowd crush. The results from these reenactments demonstrate the versatility of our

simulation framework in handling diverse scenarios and contribute to the generalizability of our approach beyond a single event. The findings also suggest that our framework can be a powerful tool for training and preparing safety officials for future mass gatherings, potentially preventing accidents.

Despite its contributions, our study has a few limitations. The current simulation employs uniform agent transition criteria that are not sensitive to terrain features, such as steep ground contacts, which may explain discrepancies in casualty distribution observed in our results. Additionally, we observed side effects, such as excessive crowd compression causing crowd surfing in articulated passive agents. We also recognize the need for improved contact responses between different types of agents to enhance stability. Moreover, the limited availability of detailed information about the Itaewon crowd crush restricts more analytic analysis, such as a fundamental diagram. Addressing these limitations will be the focus of future work.

Overall, we hope that this study provides a simulation tool for predicting and preventing crowd crushes in the future, thereby contributing to the development of effective crowd management strategies for large-scale public events.

Bibliography

[1] A. Abdelghany, K. Abdelghany, and H. Mahmassani. A hybrid simulation-assignment modeling framework for crowd dynamics in large-scale pedestrian facilities. *Transportation Research Part A: Policy and Practice*, 86:159–176, 2016.

[2] M. Choi, J. Park, and S. Ji. Risk assessments of crowds at bottlenecks through agent based modelling. *Journal of the Korean Geographical Society*, 57(6):595–609, 2022.

[3] P. Dambalmath, B. Muhammad, E. Haug, and R. Löhner. Fundamental diagrams for specific very high density crowds. *Proc. pedestrian and evacuation dynamics*, pages 6–11, 2016.

[4] T. B. Dutra, R. Marques, J. B. Cavalcante-Neto, C. A. Vidal, and J. Pettré. Gradient-based steering for vision-based crowd simulation algorithms. In *Computer graphics forum*, volume 36, pages 337–348, 2017.

[5] EDAILY. Special investigation headquarters releases cctv footage of itaewon disaster, Jan. 2023.

[6] P. Fiorini and Z. Shiller. Motion planning in dynamic environments using velocity obstacles. *The international journal of robotics research*, 17(7):760–772, 1998.

[7] R. A. Gingold and J. J. Monaghan. Smoothed particle hydrodynamics: theory and application to non-spherical stars. *Monthly notices of the royal astronomical society*, 181(3):375–389, 1977.

[8] D. Helbing and P. Molnar. Social force model for pedestrian dynamics. *Physical review E*, 51(5):4282, 1995.

[9] R. L. Hughes. A continuum theory for the flow of pedestrians. *Transportation Research Part B: Methodological*, 36(6):507–535, 2002.

[10] R. L. Hughes. The flow of human crowds. *Annual review of fluid mechanics*, 35(1):169–182, 2003.

[11] B. Lee. The october 29th itaewon disaster and state's safety measures obligation : First issue in determining whether the state compensation liability is established for the damage caused by the disaster. *Democratic Legal Studies*, 81:11–46, 2023.

[12] H. Lee. Special investigation headquarters "more than half of itaewon disaster victims endured over 408kg of force". *Weekly Chosun Magazine*, January 13 2023.

[13] R. Lohner, B. Muhamad, P. Dambalmath, and E. Haug. Fundamental diagrams for specific very high density crowds. *Collective Dynamics*, 2:1–15, 2018.

[14] A. López, F. Chaumette, E. Marchand, and J. Pettré. Attracted by light: vision-based steering virtual characters among dark and light obstacles. In *Proceedings of the 12th ACM SIGGRAPH Conference on Motion, Interaction and Games*, pages 1–6, 2019.

[15] A. López, F. Chaumette, E. Marchand, and J. Pettré. Character navigation in dynamic environments based on optical flow. In *Computer Graphics Forum*, volume 38, pages 181–192, 2019.

[16] I. Mahmood, M. Haris, and H. Sarjoughian. Analyzing emergency evacuation strategies for mass gatherings using crowd simulation and analysis framework: Hajj scenario. In *Proceedings of the 2017 acm sigsim conference on principles of advanced discrete simulation*, pages 231–240, 2017.

[17] N. Manovich and B. Sekachev. Cvat, 2024. https://www.cvat.ai/.

[18] J. Mao. A study on emergency management policy triggered by the crowd crush in itaewon, south korea. *Journal of Education, Humanities and Social Sciences*, 15:97–103, 2023.

[19] R. M. Murray, Z. Li, and S. S. Sastry. *A Mathematical Introduction to Robotic Manipulation*. CRC Press, 1994.

[20] A. Owaidah, D. Olaru, M. Bennamoun, F. Sohel, and N. Khan. Review of modelling and simulating crowds at mass gathering events: Hajj as a case study. *Journal of Artificial Societies and Social Simulation*, 22(2), 2019.

[21] K. Park. Record crowd gatherings in itaewon 1-dong... analyzing the itaewon disaster through data. *KBS News*, November 4 2022. https://news.kbs.co.kr/news/pc/view/view.do?ncd=5593479).

[22] S. Park. Social causes of disasters and the construction of meaning : The case of the oct. 29 itaewon disaster. *ECONOMY AND SOCIETY*, pages 70–100, 2023.

[23] M. Pretorius, S. Gwynne, and E. R. Galea. Large crowd modelling: an analysis of the duisburg love parade disaster. *Fire and Materials*, 39(4):301–322, 2015.

[24] J. van den Berg, M. Lin, and D. Manocha. Reciprocal velocity obstacles for real-time multi-agent navigation. In *2008 IEEE international conference on robotics and automation*, pages 1928–1935. Ieee, 2008.

[25] J. van den Berg, J. Snape, S. J. Guy, and D. Manocha. Reciprocal collision avoidance with acceleration-velocity obstacles. In *2011 IEEE International Conference on Robotics and Automation*, pages 3475–3482. IEEE, 2011.

[26] W. van Toll, C. Braga, B. Solenthaler, and J. Pettré. Extreme-density crowd simulation: Combining agents with smoothed particle hydrodynamics. In *Proceedings of the 13th ACM SIGGRAPH Conference on Motion, Interaction and Games*, pages 1–10, 2020.

[27] W. van Toll, T. Chatagnon, C. Braga, B. Solenthaler, and J. Pettré. Sph crowds: Agent-based crowd simulation up to extreme densities using fluid dynamics. *Computers & Graphics*, 98:306–321, 2021.

[28] W. van Toll, F. Grzeskowiak, A. L. Gandía, J. Amirian, F. Berton, J. Bruneau, B. C. Daniel, A. Jovane, and J. Pettré. Generalized microscropic crowd simulation using costs in velocity space. In *Symposium on Interactive 3D Graphics and Games*, pages 1–9, 2020.

[29] W. Van Toll and J. Pettré. Algorithms for microscopic crowd simulation: Advancements in the 2010s. In *Computer Graphics Forum*, volume 40, pages 731–754, 2021.

[30] L. D. Vanumu, K. Ramachandra Rao, and G. Tiwari. Fundamental diagrams of pedestrian flow characteristics: A review. *European transport research review*, 9:1–13, 2017.

[31] R. Yaagoubi, Y. Miky, K. Faisal, and A. Al Shouny. A combined agent-based modeling and gis approach for hajj crowd simulation. *Journal of engineering research*, 11(1):100014, 2023.

[32] X. Yang, H. Dong, Q. Wang, Y. Chen, and X. Hu. Guided crowd dynamics via modified social force model. *Physica A: Statistical Mechanics and its Applications*, 411:63–73, 2014.

[33] G. Yeom. A study on the improvement of the safety management of crowd accidents in the itaewon disaster. *Legal Theory & Practice Review*, 11(4):273–292, 2023.

[34] Y. Yuan, B. Goñi-Ros, H. H. Bui, W. Daamen, H. L. Vu, and S. P. Hoogendoorn. Macroscopic pedestrian flow simulation using smoothed particle hydrodynamics (sph). *Transportation research part C: emerging technologies*, 111:334–351, 2020.

[35] F. Zanlungo, T. Ikeda, and T. Kanda. Social force model with explicit collision prediction. *Europhysics Letters*, 93(6):68005, 2011.

[36] H. Zhao, T. Thrash, M. Kapadia, K. Wolff, C. Hölscher, D. Helbing, and V. R. Schinazi. Assessing crowd management strategies for the 2010 love parade disaster using computer simulations and virtual reality. *Journal of the Royal Society Interface*, 17(167):20200116, 2020.

국문초록

초고밀도 군중 키노다이내믹 시뮬레이션

: 이태원 참사 사례연구

황 주 이
인공지능 · 소프트웨어학부
이화여자대학교 대학원

본 논문은 2022년 초고밀도 군중 밀도로 인해 발생한 이태원 참사를 가상공간에서 재현하기 위해 설계된 새로운 군중 시뮬레이션 방법론을 제안한다. 제안하는 시뮬레이션 방식을 통해 군중 유체화, 군중 밀림, 붕괴와 같은 초고밀도 상황에서 나타나는 다양한 군중 행동을 효과적으로 시뮬레이션하지 못하는 기존 기술의 한계를 해결하는 것을 목적으로 하며, 이를 위해 네 가지 유형의 에이전트를 통합한 키노다이내믹 시뮬레이션을 도입한다. 본 논문에서는 환경 모델상의 에이전트의 밀도가 충분히 높지 않을 때는 에이전트의 속도를 이용한 기구학 기반의 군중 시뮬레이션을 시행하고, 고밀도일 때는 군중 유체화를 표현하기 위한 유체역학 시뮬레이션을 시행하였다. 그리고 고밀도 군중이 강한 힘을 받는 경우 관절체 동역학 시뮬레이션을 시행하여 군중의 넘어짐을 표현하였다. 서로 다른 유형의 에이전트 간의 시뮬레이션을 위해, 메시지 전달 메커니즘을 사용하여 에이전트 간 관련된 기구학 및 동역학 정보를 공유하고, 군중 밀도와 접촉력에 따라 에이전트 유형을 전환하였다.

제안된 하이브리드 시뮬레이션 결과를 CCTV 영상과 비교했을 때, 이태원 현장에서 나타난 군중 현상을 효과적이고 정확하게 재현할 수 있음을 확인하였다. 또한 ablation study를 통해 하이브리드 에이전트가 다양한 군중 행동을 재구성하는 데 있어 갖는 이점을 제시한다. 이와 함께, 재난 관리 전문가의 제안을 바탕으로 이태원 참사를 방지하기 위한 세 가지 what-if

시나리오 시뮬레이션을 수행하였다. 이 시나리오에서는 인구 유입 제한, 우측통행 적용, 좁은 골목의 불법 증축물 제거와 같은 다양한 대책을 평가한다. 연구 결과, 이러한 전략의 조합이 군중 흐름을 크게 개선하고 고위험 밀집도를 완화하는 데 효과적임을 확인하였다. 마지막으로, 제안된 방법의 다양성과 적용성을 입증하기 위해 Love Parade 2010과 Oasis Concert 2005와 같은 두 가지 실제 군중 사고를 재현하였다. 이 재현 사례는 다양한 군중 상황에서 하이브리드 시뮬레이션 프레임워크의 적용 가능성을 보여주며, 대규모 행사의 군중 패턴 예측 및 군중 안전 관리 전략 설계 도구로서의 잠재력을 보인다.